Article

A Feasible Proposal for Energy-Efficient Roof Retrofitting in Southern European Obsolete Residential Neighborhoods

Carlos-Antonio Domínguez-Torres [1,2], Helena Domínguez-Torres [3,4], Miguel Hernández-Valencia [5,6], Jorge Roa-Fernández [5,7] and Rafael Herrera-Limones [5,6,*]

1   Escuela Técnica Superior de Arquitectura, Universidad de Sevilla, Avda.Reina Mercedes 2, 41012 Sevilla, Spain; cdtorres@us.es
2   Research Group TEP130, Universidad de Sevilla, 41012 Sevilla, Spain
3   Facultad de Ciencias Económicas y Empresariales, Universidad de Sevilla, Avda.Ramón y Cajal, 1, 41018 Sevilla, Spain; hdtorres@us.es
4   Research Group SEJ490, Universidad de Sevilla, 41012 Sevilla, Spain
5   Instituto Universitario de Arquitectura y Ciencias de la Construcción, Escuela Técnica Superior de Arquitectura, Universidad de Sevilla, Av. Reina Mercedes 2, 41012 Sevilla, Spain; mhvalencia@us.es (M.H.-V.); jroa@us.es (J.R.-F.)
6   Research Group HUM 965, Universidad de Sevilla, 41012 Sevilla, Spain
7   Research Group TEP 206, Universidad de Sevilla, 41012 Sevilla, Spain
*   Correspondence: herrera@us.es

Abstract: 1960s Europe saw a large number of residential neighborhoods built to house those migrating from the countryside. Today, more than 50 years later, these neighborhoods suffer high levels of functional, social, and technical obsolescence. In response to this, the University of Seville developed the Aura Strategy as an intervention methodology to find global solutions to issues in outdated neighborhoods. To provide visibility to this aspect of the Aura Strategy, the retrofit proposal presented in this article provides a solution to improve the roofing of buildings in a case study neighborhood (Polígono de San Pablo, Seville) and an analysis of the results in terms of energy and financial savings for local residents. The results show that for a population of roughly 18,000 (in 2018), net savings, including energy and retrofitting costs, ranging from nearly €6.5 to over €8.6 million can be made over the 20-year life-cycle span. Likewise, the results obtained on the reduction of thermal loads indicate a 72% decrease in energy consumption, equivalent to a saving of close to 4500 tons of greenhouse gas emissions for the district and the entire life-cycle time period, with the consequent benefits on the impact on air quality and the fight against climate change.

Keywords: urban sustainability; social construction; retrofit energy saving measures; aging effect; thermal dynamic model; numerical methods; life cycle cost analysis

1. Introduction

The neighborhoods built in Europe during the 1950s and 1960s in response to the mass migration of workers from the countryside to cities need rehabilitation. To do so, architectural retrofitting should be considered rather than demolition or new construction. To reduce the carbon footprint of the process, the intervention strategy in these outdated neighborhoods should be based on methodologies that enable the refurbishment and transformation of buildings through the conservation and reuse of the existing urban fabric instead of demolition and the generation of new buildings. This is the intervention methodology proposed by the Aura Strategy. This strategy has been developed by a group of researchers from the University of Seville and has been tested in various editions of the Solar Decathlon competition [1,2]. It is currently being applied in the Polígono San Pablo neighborhood within the framework of the "Direct application of the SOLAR DECATHLON-U.S Team Aura Strategy in the rehabilitation of obsolete Andalusian neighborhoods" research project financed by the regional government of Andalusia, Spain. The

Aura Strategy is an "urban acupuncture strategy" that proposes a gradual requalification of social identity, material, and energy, ensuring an effective improvement in the health and comfort of residents, leading to an increase in quality of life. The Aura Strategy proposes actions centered on four lines of intervention. These are:

- Comfort and Health
- Materiality
- Cultural Identity and Accessibility
- Retrofitting and Energy

The neighborhood of Polígono de San Pablo was selected for this study because it is an obsolete residential neighborhood, included in the Catalogue of Vulnerable Neighborhoods (VN) in Spain 2011 [3]. A Vulnerable Neighborhood is defined as an urban area of a certain homogeneity and urban continuity, delimited on the basis of an area of between 3500 and 15,000 inhabitants in which at least one of the three Basic Indicators of Urban Vulnerability (BIUV; BIUV Studies, BIUV Housing, or BIUV Unemployment) exceeds a value established as a vulnerability reference.

The Aura Strategy is also applicable to other locations. For its application to other locations, the strategy is always based on a previous analysis of energy, materiality, social and cultural aspects, or identity. In this way, the response and actions can be adapted to specific and different locations, climates, and environments. The strategy is not the material solution but the methodology that determines this solution.

This article examines the line of materiality and centers on one of the most evident weaknesses present in the buildings of this case study neighborhood: roofs. The aim of this research is to use a dynamic time-dependent analysis of the energy and economic variables of the life-cycle time span and to propose and assess a retrofit solution for the roofing of the buildings in the neighborhood of Polígono de San Pablo. This refurbishment solution is implemented with the purpose of reducing the energy consumption required to provide thermal comfort conditions in homes on the top floor, with the consequent benefits in the reduction of energy poverty, which has such a strong impact on the social context under study, while at the same time, through the consequent reduction of greenhouse gases, it implies important benefits for air quality and the fight against climate change.

1.1. Passive Roofs Strategies

On a typical hot sunny day in the summer, as they usually are under mediterranean climate conditions, building rooftop surfaces can be 27–50 °C hotter than the surrounding air temperature [4], which means that the heat transmitted by convection to the surrounding air and by thermal radiation to taller buildings can be very significant and contributes to urban heating and the so-called Urban Heat Island effect. Therefore, reducing the temperature of the rooftop influences the improvement of the quality of the urban environment [5] at the same time that it reduces the cooling loads necessary to obtain internal thermal comfort conditions [6], which in turn reduces the rejection of heat from heating systems, further strengthening the urban heat island while producing a decrease in greenhouse gas emissions through the reduction of energy consumption.

A large body of research has been conducted for generating strategies for roof heat mitigation with multiple approaches, among which passive strategies are especially interesting in the context of this work.

The role of the inclination and orientation of the rooftop was analyzed in [7] for lightweight and heavyweight roofs equipped or devoid of an insulation material during the cooling period in Italy and Greece.

Different insulation materials in arid zones were studied in [8], where four different structures to cool the roof in Jordania were analyzed and it was found that clay thermal insulation over the roof provided the best results for cooling of the building for better comfort conditioning in arid areas.

In [9], using thermal models created with Energy Plus, the authors concluded that the use of cool roofs resulted in a 17% drop in the annual cooling demand for the building investigated in the urban region of Acharnes municipality in Greece.

In [10], exploring the possibilities of energy savings, the research examined the effectiveness of dynamic cool roofs (DCRs) incorporating seasonally variable reflective surfaces across different building prototypes in comparison to static cool roofs. wherein the authors found that applying variable reflective coatings to buildings with low insulation levels can result in source energy savings, ranging between 4.33 and 19.44 MJ/m^2 (or 1.6–4.9%) for residential units and 1.17 and 18.00 MJ/m^2 (equivalent to 0.3–3.9%) for office structures.

In [11], through the application of building energy simulation, the investigation focused on isolating the consequences of enhancing rooftop radiative properties on surface temperatures and heat fluxes. The results suggest that elevating rooftop solar reflectance from 0.2 to 0.96, with a fixed emissivity of 0.9, leads to an average reduction in rooftop temperature of approximately 10 °C.

In [12], the effect of the installation of an innovative cool clay tile on the rooftop of historic residential buildings in central Italy was analyzed, and they found maximum primary energy saving for cooling about 51%, while the heating energy penalty was slower than 2%.

A ventilated roof is proposed and implemented in [13] as a passive cooling technique that allows environmental heat sinks such as night ventilation and evaporative cooling. Energy impact analysis showed that implementing the ventilated roof solution can reduce cooling needs by 65% without a resulting heating penalty.

In [14], different urban surface parameters were evaluated from several perspectives to assess their comparative effectiveness as heat mitigation strategies and concluded that roofs with high albedos are found to be the best heat mitigation for reducing daytime temperatures (0.85 albedo, 1.29 °C) while green roofs show the best nighttime efficacy (100%, 1.15 °C).

In [15], three different cooling roof techniques were addressed: cool reflective white paint, white ceramic tiles, and a cool-ventilated roof. These techniques were analyzed by monitoring both roof surface temperatures and indoor temperatures. It was concluded that a cool-ventilated roof is the most efficient solution, reducing the average indoor temperature by 4.95 °C.

In [16], the aging characteristics of high solar reflective index (SRI) or cool paints were assessed qualitatively, and the energy savings for their application in residential buildings were estimated.

Diurnal Selective Radiative Cooling based in roof panels RC roofs was studied in [17], where it was found that in terms of surface temperature, RC panels outperformed high performance cool roofs, but in terms of anthropogenic heat reduction and microclimate air temperature reduction, they both had a similar impact.

In [18], a literature review is conducted and a general framework is proposed that allows current modeling to go beyond typical protocols by including data relating a specific urban microclimate at the neighborhood/city level to that of a building, thus linking the environmental microclimate to the objective appraisal of building energy efficiency.

On the other hand, in the framework of the Mediterranean climate, one of the proven effective measures to save cooling energy is through the use of a suitable combination of thermal insulation and a rooftop coating highly reflective of solar radiation; this combination, when well designed, has proven to provide significant savings energy to achieve thermal indoor comfort and to be cost efficient [19,20]. This combination of thermal insulation and cool coating is the constructive solution used here to retrofit the roof of the case study buildings considered in this work.

Regarding the agreement of the results obtained in the present research with the previous literature, it can be said that for the energy and cost analyses, the results are consistent with the findings presented in [6,20] for the case of a single roof, without entering into a neighborhood context that is not addressed in these works cited.

1.2. The Case Study Approach

Construction of the Polígono de San Pablo began in the year 1961. Around 57,000 people were expected to live there, divided into five districts (A, B, C, D, and E), each with 2000 homes, as seen in Figure 1. This research aims to quantify the relevance of planning a comprehensive intervention that covers all five districts of the neighborhood.

The neighborhood includes different types of 4, 8, and 12 storey residential buildings. Among these, there are 707 free-standing buildings and an estimated 112,000 m^2 of roof area, Figure 2. Considering that most building types are two homes per floor, 1414 homes will benefit directly from this intervention. In other words, all of the top-story homes in each retrofitted building. The typical building roof plan is shown in Figure 3. This is a conventional typology of walkable roof with a ceramic coating.

Figure 1. Districts of the Polígono de San Pablo neighborhood.
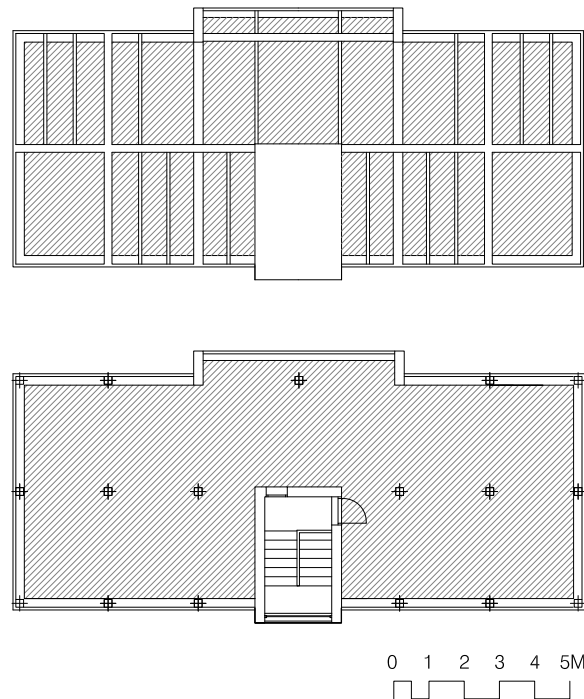

Figure 2. Aerial photo taken using UAV technology.

Figure 3. Roof plan.

2. Materials and Methods

2.1. Methodology for Energy Computation

This section outlines the methodology followed to evaluate the thermal energy crossing the roof. First, the physical assumptions are presented, then, the associated mathematical equations are shown, and finally, the aging effect for the retrofitted roof and its practical implementation are described.

2.1.1. Physical Framework

In this section, the physical framework involving the heat flux through the roof is described. Specifically, thermal flux through the roofs is determined by the following:

- Thermal gains due to solar radiation impacting the roof's outer surface.
- Infrared radiative heat transfer between the roof's outer surface and the open sky and taller buildings.
- Convective heat transfer between the roof's exterior surface and the surrounding air.
- Conduction-based thermal transfer within the roof's multiple layers.
- Convective heat transfer between the roof's interior surface and the indoor air.
- Infrared radiative heat transfer between the roof's inner surface and the room indoor surfaces.

Section 2.2.2 provides details on how to compute the solar radiation absorbed by the roof's outer surface. This result is based on the solar radiation values obtained from climatic data, such as the Energy Plus Weather (EPW) files, or from monitoring data that are entered into the model. When computing the solar radiation gain, it is important to consider the absorptivity of the outer surface. As it is subject to the so-called ageing effect, it is non-constant in time. The pattern of change in the solar absorptivity of the outer surface of the roof is described in Section 2.3.

The radiative heat exchange between the outer surface of the roof and the sky is computed by calculating the downward horizontal infrared radiation intensity through the use of the sky emissivity as described in Section 2.2.3.

The convective heat transfer between the outer surface of the roof and the surrounding air is calculated by a two-fold approach: on the one hand, using convective heat transfer correlations to calculate the energy balance on the outer surface of the roof, and, on the other

hand, by calculating the thermal boundary layer of the air on the roof. Both procedures are described in Section 2.2.4.

To estimate the heat transfer by conduction through the different layers of the roof, the physical model is based on the models of thermal conduction through a multilayer wall considering the different thermophysical values of each layer that makes up the roof as described in Section 2.2.5.

Finally, the infrared radiative and convective heat transfer between the roof's inner surface and the building indoor is carried out using a combined convective-radiative transfer coefficient applied to the energy balance on the inner roof surface as described in Section 2.2.5.

2.2. Mathematical Formulation

In this section, drawing on the physical principles established in the earlier section, we bring forth the mathematical equations relevant to heat transfer across the roof.

2.2.1. Energy Balance on the Outer Roof Surface

As a result of the energy processes taking place on the outer surface of the roof listed in Section 2.1.1, an energy balance is produced on that surface. This balance can be represented by the equation:

$$\kappa \frac{\partial T_{S_{ext}}}{\partial \vec{n}} + \dot{q}_{conv,ext} + \dot{q}^{SW} + \dot{q}^{LW} = 0 \tag{1}$$

where $\vec{n}$ is the outward normal vector to the roof external surface S_{ext}; κ is the conductivity of the material composing S_{ext}, and $T_{S_{ext}}$ is the temperature on surface S_{ext}; $\dot{q}_{conv,ext}$ is the intensity of convective heat flux between S_{ext} and the ambiance air; $\dot{q}^{SW}$ is the intensity of the solar radiation flux reaching S_{ext}; $\dot{q}^{LW}$ represents the balance of thermal radiation between S_{ext} and the sky and surroundings.

2.2.2. Absorbed Solar Radiation Calculation

Regarding solar radiation, a relevant quantity for the computation of the thermal flux through the roof is the quantity of solar energy absorbed by the roof surface facing outward, that is computed here as:

$$\dot{q}^{SW} = \alpha^{SW} \cdot \left(I_b \cdot cos(\theta) \cdot \frac{S_s}{S_{roof}} + I_{sd} \cdot F_{rs} + I_{gd} \cdot F_{rg} + I_{rn} \cdot F_{rn} \right), \ [\text{W/m}^2] \tag{2}$$

where α^{SW} represents the solar absorptance coefficient of the roof's outermost layer, θ denotes the solar beam's angle of incidence on the roof, I_b is the intensity of the normal direct solar radiation, S_s is the sunlit area of the external roof surface, S_{roof} is the entire roof area, I_{sd} and I_{gd} are the reflected diffuse solar radiation intensity from the sky and the ground, F_{rs} is the view factor roof-sky, F_{rg} is the view factor roof-ground, I_{rn} represents the intensity of radiation reflected by the nearby buildings or any other vertical object such as trees, and F_{rn} represents the view factor between the roof and the neighboring objects.

When there are no structures or shading elements surpassing the specified roof in height, F_{rs} and F_{rg} are given by

$$F_{rs} = \frac{1 + cos(\varphi)}{2}, \qquad F_{rg} = \frac{1 - cos(\varphi)}{2}$$

where φ is the angle that defines the tilt of the roof plane relative to the horizontal plane. In the case of an unshaded horizontal flat roof, φ is equal to 0 and Equation (2) becomes

$$\dot{q}^{SW} = \alpha^{SW} \cdot I_H, \quad [\text{W/m}^2], \tag{3}$$

where I_H is the intensity of the global horizontal solar radiation reaching the roof that is given by

$$I_H = I_b \cdot cos(\theta) + I_{sd}. \tag{4}$$

2.2.3. Long-Wave Radiative Exchange with the Sky

The long-wave radiative exchange between the external roof surface and the sky is calculated using the expression

$$\dot{q}^{LW} = \dot{Q}_{sky}^{LW} - \dot{Q}LW_w$$

where $\dot{Q}_w^{LW}$ is the intensity of the thermal long-wave radiation emitted by the external roof surface and $\dot{Q}_{sky}^{LW}$ is the sky downwelling long-wave radiation.

$\dot{Q}_w^{LW}$ is calculated using the Stefan–Boltzmann law:

$$\dot{Q}_w^{LW} = \epsilon_w \sigma T^4 \tag{5}$$

where ϵ_w and T are the emissivity and the temperature in Kelvin degrees of the external surface of the roof, and σ is the Stefan–Boltzmann constant given by $\sigma = 5.67 \cdot 10^{-8}\ [W/m^2\,K^4]$.

To compute the sky downwelling long-wave radiation $\dot{Q}_{sky}^{LW}$, following [21,22], the correlation used is:

$$\dot{Q}_{sky}^{LW} = \epsilon_{sky} \sigma T_{ext}^4, \tag{6}$$

where ϵ_{sky} is the sky emissivity and T_{ext} is the ambiance dry-bulb temperature in Kelvin degrees. From the same references [21,22], ϵ_{sky} is computed by

$$\epsilon_{sky} = (0.787 + 0.764 \ln(\frac{T_{dp}}{273}))(1 + \frac{224}{10^4}n - \frac{35}{10^4}n^2 + \frac{28}{10^5}n^3)$$

where n is the opaque sky cover in tenths and T_{dp} is the dew point temperature in kelvin degrees. This approach is the same used by some well-known software of Building Energy Simulation as Energy Plus [23].

2.2.4. Heat Exchange between the Roof and the Ambiance Air

The heat exchange between the roof and the ambiance air, $\dot{q}_{conv,ext}$ in Equation (1), is one of the processes that most affects the thermal behavior of the roof, hence the need to explore ways to ensure the accuracy of the calculation of this process.

In this work, two ways of estimating $\dot{q}_{conv,ext}$ have been analyzed. The first is a typical approach based in the use of convective heat transfer coefficients $h_{conv,ext}$. The coefficient $h_{conv,ext}$ used here is based in the work of Hagishima and Tanimoto [24] and was obtained from experimental measurements on building roofs. The obtained correlation was

$$h_{c,ext} = 8.18 + 2.28\,V_R \quad [W/m^2K], \tag{7}$$

where V_R expresses the wind velocity above the roof, measured in meters per second. Then, the convective heat flux is given by

$$\dot{q}_{ext} = h_{c,ext}(T_{ext} - T_{S_{ext}}), \quad [W/m^2]. \tag{8}$$

In the second approach used to estimate the heat exchange between the roof and the ambiance air, no external convective heat transfer coefficient has been used. Instead, the air flow over the roof has been modeled using the Navier–Stokes thermodynamic equations together with a turbulence modeling using the well-known $\kappa - \varepsilon$ model. From these equations, the velocity and temperature of the air in the boundary layer adjacent to the outer surface have been determined. Then, the value thus calculated for the air temperature in the zone of the thermal boundary layer closest to the roof surface is the one used to determine the heat exchange $\dot{q}_{ext}$.

To carry out this modeling of the air flow over the roof, a parabolic air profile, used in energy performance of buildings [25], has been considered in the input of the calculation domain:

$$V(h) = V_r \left(\frac{h}{h_r} \right)^\gamma \quad \text{(m/s)} \tag{9}$$

In this equation, $V(h)$ represents the wind velocity at height h, V_r denotes the wind speed measured at the reference altitude h_r, and γ is a coefficient that varies depending on the local orographic and roughness characteristics.

The remaining border conditions for air velocity are non-slip velocity on the outer roof surface, slip condition on the top of the domain, and finally, free outflow in the outlet boundary surface.

2.2.5. Heat Conduction through the Roof

The conduction of heat through the roof can be modeled as a specific case of diffusion through a multilayer wall [26] and employing boundary conditions as defined by the energy balance equations for both the exterior and interior surfaces of the roof.

The boundary conditions for the roof outer surface are described in Equation (1) and Section 2.2.4.

Regarding the roof's interior surface, when conducting the energy balance analysis for this surface, a mixed convective-radiative transfer coefficient $h_{conv,rad}$ was used. Here, following the values recommended by [27], the values considered for this coefficient were $h_{conv,rad} = 9.26 \, [\text{W/m}^2\text{K}]$ for upward heat flux and $h_{conv,rad} = 6.13 \, [\text{W/m}^2\text{K}]$ for downward heat flux.

Finally, the model approximation for the simulation of the heat through the roof is the model for heat conduction through a multilayer wall introduced in [28], which is based on an approximation that takes into account specific continuity conditions between layers for temperature and heat flux.

2.3. Changes in Cool Roof Reflectivity Due to Aging

It has been established in the previous literature [29–33] that cool coatings, based on paints or elastomeric materials, are affected by an aging effect that alters their solar reflectivity. The thermal performance of roofs is significantly impacted by this aging effect, as indicated in [6]. In this last work, the comparison between the heat flux through a roof considering the aging effect and the same roof without taking this effect into account showed a significant difference that can lead to erroneous estimates of energy consumption and the results of the economic cost effectiveness analysis of energy retrofit measures on roofs. Therefore, when calculating heat flux through roofs, this aging effect must be taken into account and included in its energy calculation to draw reliable conclusions. In conclusion, to simulate realistic conditions, the aging effect must be considered to draw accurate conclusions with respect to the energy and economic outcomes of the retrofitted roofs.

To account in the energy calculations for this aging effect, the first stage is to establish the pattern of aging. In [32], it was shown that for all types of reflective roof coatings tested, in the early two years after installation, roughly 95% of aging happened, with 98% occurring within the first three years after installation; similarly, research has demonstrated that when considering unwashed cool roof coatings on various substrates, there is typically a decrease in initial solar reflectivity of approximately 20–25% within the first few months to one year, with minimal alterations thereafter, and substrate type typically has limited impact. On the other hand, Bretz and Akbary [33] found that the majority of the decline in solar reflectivity takes place within the initial year, potentially even within the first few months, and then the value of solar reflectivity tends to remain stable. Eilert [34] also illustrated that the decline in solar reflectivity of white roofs is in the order of 10–30% and the greatest decrease typically occurs during the first year. Based on the field survey [32], the recommendation is to perform energy calculations using reflectivity values aged for a minimum of one year, which usually range from 75% to 80% of the initial values.

A similar conclusion was reached in [29]. The study's field measurements yielded results indicating a decrease in solar reflectance ranging from 19% to 25% for various cool paints. In this study, it was also noted that the aging of the cool coating layer has a minimal impact on its thermal reflectivity.

On the other hand, field measurements [32,33] suggest that periodic washing can reinstate the original reflectivity values to 90–100%. Nonetheless, as indicated by the author of this field research, the use of roof washing as a maintenance strategy for cool-coated roof surfaces is not a cost-effective approach for retaining or renewing solar-reflectance values, especially given the expectation that most solar reflectance loss will reoccur within three to six months. While washing can typically renew most of the solar reflectivity, especially during the early aging years, the effects are temporary (typically for three to six months) and deliver limited economic benefits.

According to the consensus in most of the studies we have examined, the aging trend considered for the cool roof coating is as follows: during the first year, there is a reduction in solar reflectivity amounting to 20% of its initial value, with the majority occurring in the initial months of the year, and a further loss of 8.5% in the second year. A reduction of 0.9% is expected for the third year. Afterwards, the drop in reflectance tends to become steady [33], resulting in a total loss of 30% over the complete life cycle. Therefore, as indicated in [32], nearly 95% of the aging takes place within the initial two years, and approximately 98% occurs during the first three years after installation.

On the other hand, when a wash is performed some years after installation, the relating literature supports that solar reflectivity is restored to 90% of the initial value. Subsequently, we consider the same pattern observed after the initial application of the cool coating.

The solar reflectivity loss considered in this work as a result of the aging effect is estimated following the aforementioned aging patterns. In Figure 4, the estimated percentage of reflectivity loss for each year is shown.
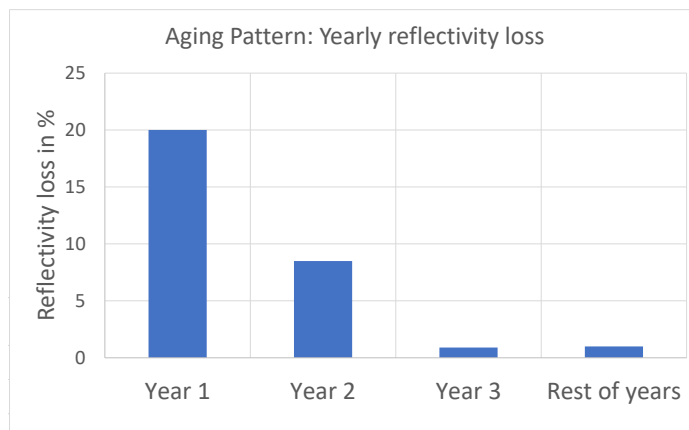

Figure 4. Pattern of solar yearly reflectivity loss in %.

2.4. Roof Energy Calculation

Case Buildings

In this study, we considered a typical building from the social housing edified in Seville before 1979. The analyzed building belongs to a social housing development named Polígono de San Pablo, built in the city of Seville, Spain, in the decade of the 1960s. This development showcases the typical construction style seen in social housing throughout this era, where the absence of energy insulation measures is a prominent feature.

The roofs, as shown in Figure 2, are of the flat type. The development is made up of equal height buildings, and there are no adjacent structures of superior elevation that could cause shading over the roofs analyzed. Thus, the solar radiation flux reaching the roofs can be described by Equation (3).

Figure 5a shows the layout of the roofs, while, in Table 1, the thermophysical values and dimensions of the roof layer are described. These types of roofs will be considered as the reference roofs to quantify the energy reduction obtained from implementing the retrofit measure. The data presented in this table correspond to the nominal values and were based on [35].

The reference roof is coated with a layer of bituminous paint on its outer surface. Consequently, a solar radiation absorptivity coefficient equal to 0.8 has been considered in line with typical absorptivity values for this coating type [36].

Table 1. Thermophysical characteristics of the reference roof.

Layer	Description	Thickness (m)	Density (kg/m^3)	Specific Heat (J/kg K)	Conductivity (W/m K)
1 (Ext.)	Bituminous paint	0.0015	1150	1000	0.23
2	Ceramic tiles	0.005	2000	800	1.00
3	Mortar	0.01	2000	1000	1.40
4	Protective layer	0.015	1150	1000	0.23
5	Mortar	0.01	2000	1000	1.40
6	Carbon cinders	0.1	640	657	1.40
7	Concrete vault	0.22	1330	1000	1.32
8 (Int.)	Gypsum plaster	0.01	1000	1000	0.32

The energy retrofit measure proposed for the obsolete energy reference roof is a combined measure consisting of the installation of 0.08 m thick EPS insulation with the addition of an external coating of cool, white elastomeric paint, featuring an absorptivity value of 0.1. These values were taken based on a previous study [20] on the thermal performance of this type of combined energy retrofitting measures, which showed that the referred values give very good energy and economic results as demonstrated by a cost-effectiveness analysis conducted for the whole life cycle of the retrofitting measure.

Figure 5b illustrates the proposed retrofitted roof layout, while Table 2 includes the dimensions and thermophysical values. The data shown in this table correspond to the nominal values and were based on [35] and specifications from manufacturers.

The analysis of the energy and economic performance of the roof involves optimizing the combination of insulation thickness and the absorptivity value of the cool paint while considering the previously discussed time-varying reflectivity of the cool coating.

Table 2. Thermophysical properties of the retrofitted roof.

Layer	Description	Thickness (m)	Density (kg/m^3)	Specific Heat (J/kg K)	Conductivity (W/m K)
1 (Out.)	White elastomer	0.0015	1150	1000	0.23
2	Regularization layer	0.01	2000	1000	1.40
3	EPS	0.08	30	1210	0.04
4–10 (Int.)	Same as layers 1 to 7 of the reference roof (Table 1)				

Figure 6 shows the climatic chart for Seville, whose values are collected from information sourced from the Spanish Governmental Meteorological Agency (AEMET) [37]. According to the referred data, throughout the year, the temperature averages 19.2 degrees Celsius, with July and August experiencing maximum averages of 40 degrees Celsius, and January registering a minimum average of 5.7 degrees Celsius.
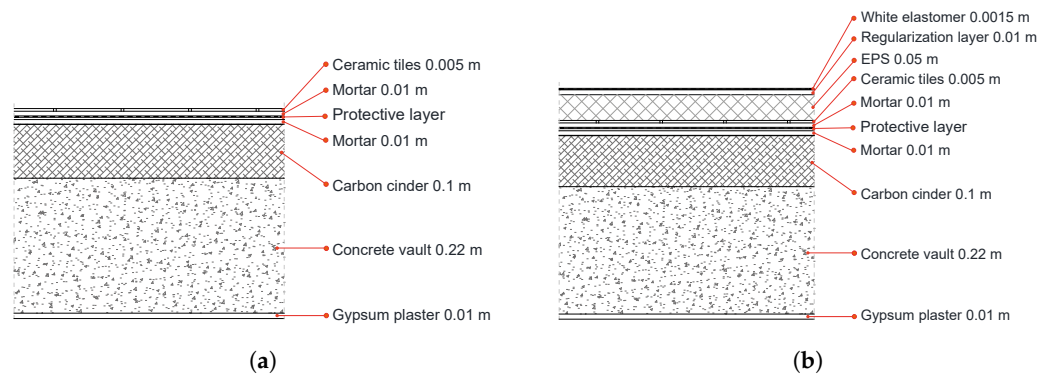
Figure 5. Layout of (**a**) the reference roof; (**b**) the retrofitted roof.
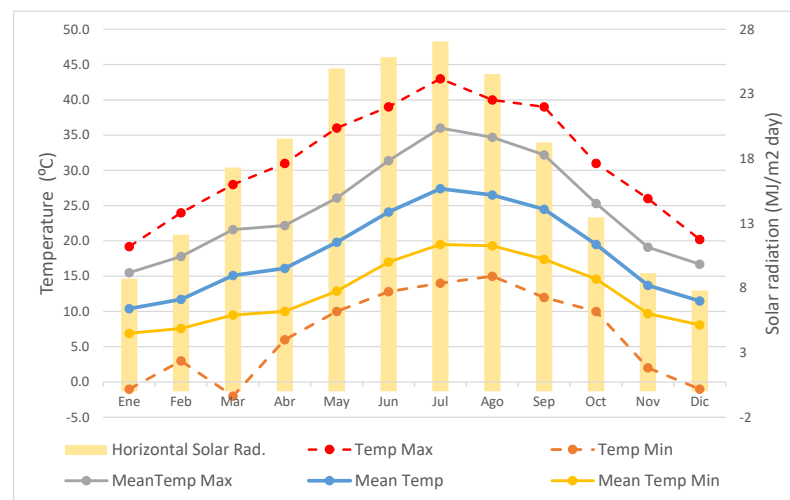

Figure 6. Climatic chart of Seville.

Thus, winter can be defined as mild, with summers being hot, dry, and experiencing high levels of solar radiation. Lastly, autumns and springs see rainfall along with moderate temperatures. The normal solar radiation reaches its peak at 8.3 kWh/m^2 in July and it decreases to a minimum of 2.3 kWh/m^2 in December. Considering the described meteorological values, the Köppen–Geiger climate classification system identifies the region's climate as Mediterranean Csa.

2.5. Numerical Resolution

The spatial approximation to the equation governing the heat transfer across the roof was based in the 1D finite difference scheme introduced and validated in [28]. To perform the entire computation process, a code was developed using the *FreeFem++* software [38].

In the approach that uses Navier–Stokes thermodynamic equations to determine the heat exchange between the roof and the ambiance air, the numerical resolution of the governing equations for the external air and the equations for the heat conduction through the roof were performed in a coupled way.

Since, as can be seen in Figure 2, buildings can have different orientations, a sensitivity analysis of the influence of building orientation on heat transfer through the roof was first performed. This preliminary analysis was performed using a 3D approximation of the thermodynamic airflow equations and showed that the changes in heat transfer through the roof due to building orientation were negligible, with the difference between all the orientations considered being less than 0.6%. This made it possible to solve the Navier–Stokes equations using a 2D approximation where the relevant variable for the dynamic of the air was the wind velocity.

As for the approach using the convective heat transfer coefficient, the heat exchange between the roof and the outside air is calculated using Equation (8) and using the value obtained from the energy balance Equation (1) on S_{ext}, which is the boundary condition on the outside surface of the roof for the numerical method that calculates the heat transfer through the roof.

With respect to the impact on the heat flux through the roof, a difference of less than 1% was observed between the two approaches used for the calculation of the convective flux with the ambiance air, a difference that may make it advisable to use the convective correlation methodology for the present case due to its greater simplicity of use and lower computational cost.

The numerical model validation process was carried out, following [6], in a twofold way: first, through an inter-model comparison and second, through an analytical validation.

This way, to evaluate the accuracy of the proposed numerical scheme, an inter-model validation was first performed by comparing the model results with the results obtained from the Energy Plus software [23]. This was executed by adopting short time spans for the calculation, typically in the order of months due to the fact that time-dependent solar reflectivity is not supported by Energy Plus, as it is built to accommodate only constant values of solar reflectivity. It should be noted that in the developed numerical model, the change in time of the solar reflectivity was implemented in order to enable the simulation of the impact of aging on cool roof absorption over extended time frames, often spanning decades, as applied in our Life Cycle Cost Assessment (LCCA) calculations.

In addition, from a numerical perspective, we validated the method through analytical calculations of temperature evolution at the nodes employed in the finite difference method. These calculations utilized a limited number of nodes for roof discretization [39].

The model calculation of the energy flux through the roofs showed a good fit with the estimated values following the two ways of validation indicated, obtaining a relative error of less than 8% when compared to the energy flux values from the Energy Plus model, and less than 5% for the comparison with the analytical solution. More details on the validation procedure can be found in [6,20].

Within the interior zone beneath the roof, our approach involves a test zone that draws inspiration from [19,40,41], with the underlying assumption that the building envelope is adiabatic, except for the roof.

The roof's thermal response is determined by the conditioning system's operational mode. Several operational modes are documented in the literature, encompassing continuous air conditioning [19,42–45], intermittent air conditioning with a consistent indoor set-point temperature [46], and no air conditioning with indoor temperature variations [47]. When examining the energy behavior of the roof and its implications for energy consumption, we make the assumption that the ambient indoor temperature remains uniform for each season.

We consider a continuous mode of operation for the conditioning system, with the indoor set-point temperature set at 25 °C during the cooling season, 20 °C during the heating season, and 22.5 °C during the seasons in between. These values have been chosen while keeping in mind the comfort temperature intervals defined in the Spanish regulation for thermal installations in buildings (RITE) [48].

Finally, two maintenance scenarios were considered: the first assumed that a powerful washing of the cool coat is not performed, and the second assumed a powerful washing of the roof with a periodicity of five years. This periodicity, according to [21], achieves very positive outcomes from both energy and economic viewpoints. On the other hand, as is supported in the relating literature cited in Section 2.3, if a wash is performed some years after the installation, the solar reflectivity is restored to 90% of its original value. In the aftermath, we follow the same pattern as seen following the initial application of the cool coating.

2.6. Methodology for the Life Cycle Cost Analysis

To perform an economic analysis of the energy and retrofit costs and draw conclusions about its financial suitability, the usual approach is to carry out a cost-effectiveness analysis through a Life Cycle Cost Analysis (LCCA) that considers future costs [49]. Therefore, the objective of the LCCA performed in this section is to evaluate the economic benefits of the proposed roof retrofit measure compared to the reference case.

Using the method introduced in [49], it is possible to establish a comparison of future costs with current costs and, in addition, to obtain the savings obtained by using the retrofitted roof over the life-cycle time span. To perform the LCCA, anticipated costs are estimated and then discounted to reflect their present value. For this, we account for the future values of the elements that drive the costs; then, each annual variable cost is discounted to reflect its current value. Finally, the LC cost is the sum of the present values for all variables involved in the study. Once the LC cost for the retrofitted roof has been determined, its cost effectiveness is assessed by comparing this cost with the LC cost obtained for the reference case. If the LC cost produced by the retrofitted roof is lower than that caused by the reference case, the retrofitted roof is considered cost-effective and yields positive monetary savings.

To perform the LCCA, a lifetime equal to 20 years is considered; this is the average service life of the retrofit measures considered [50]. Then, the LC cost, the LC monetary savings or net cost savings (NCS), and the return-on-investment period or payback period (PB) are estimated for the retrofitted roof. The variables involved in this analysis are the initial investment cost of installing the reflective coating and the thermal insulation layer, the annual costs of energy, and the maintenance costs of the periodic washing of the cold roof coating, along with the economic parameters that influence the economic process: the monetary discount rate dr and the increase in energy costs index i. In order to calculate the current value of one monetary unit of a future period m (typically measured in years) at a market discount rate dr (expressed as a fraction per time period), the applicable formula is as follows

$$PW_m = 1/(1+dr)^m \, .$$

Assuming that $P_{e,C}$ and $P_{e,H}$ denote the current energy prices for cooling and heating, and that i is the energy cost inflation rate index, the present value of the future energy cost $C_e(m)$ in the period m is given [49] by

$$PW_m(C_e(m)) = C_e(m)/(1+dr)^m$$

being

$$C_e(m) = \left(\frac{Q_c(m) \times P_{e,c}}{SEER \times (3.6 \times 10^6)} + \frac{Q_h(m) \times P_{e,h}}{SCOP \times (3.6 \times 10^6)} \right) (1+i)^{m-1} \tag{10}$$

with SEER representing the seasonal energy efficiency ratio for cooling and SCOP denoting the seasonal performance coefficient for heating of the conditioning equipment in use. In Equation (10), it is considered that the loads $Q_c(m)$ and $Q_h(m)$ for the cool roofs fluctuate annually as a result of both aging and the maintenance applied to the cool coating. $C_e(m)$ calculations always assume the use of electricity for cooling and heating.

Similarly, if the inflation rate index for maintenance costs is noted as i_M, the current worth of any forthcoming maintenance payment $C_M(m)$ in time period m is

$$PW_m(C_M(m)) = C_M(m)/(1+dr)^m = \delta(m) \, C_M(1+i_M)^{m-1}/(1+dr)^m$$

where $\delta(m)$ is equal to 1 if maintenance is done in year m or equal to 0 if not, C_M is the current price of maintenance per unit area of roof surface and A is the area of the roof surface.

Next, the current life-cycle total cost per unit of roof surface area is provided as follows:

$$C_t = C_e + C_M + C_I$$

where C_e and C_M refer to the present worth of the overall life-cycle costs for energy and maintenance, respectively, as determined by

$$C_e = \sum_{k=1}^{n} PW_k(C_e(k)) \quad \text{and} \quad C_M = \sum_{k=1}^{n} PW_k(C_M(k)).$$

Lastly, C_I represents the expense associated with the initial investment of cool roof coating installation.

In contrast to the initial reference roof, the retrofit will bring about annual changes in energy usage and the corresponding economic adjustments, primarily linked to energy costs. To determine the cost differential between employing cool roofs and the reference case, we calculate the net cost savings (NCS) for the entire life-cycle period using the following expression

$$NCS = \sum_{m=1}^{n} \left[PW_m(C_e^{(ref)}(m)) - PW_m(C_e(m)) \right] - C_M - C_I, \tag{11}$$

where now $PW_m(C_e^{(ref)}(m))$ represents the current value of energy costs for the roof reference case at period m, determined as:

$$PW_m(C_e^{(ref)}(m)) = C_e^{(ref)}(m)/(1+dr)^m,$$

where $C_e^{(ref)}(m)$ is computed as

$$C_e^{(ref)}(m) = \left(\frac{Q_c^{(ref)}(m) \times P_{e,c}}{SEER \times (3.6 \times 10^6)} + \frac{Q_h^{(ref)}(m) \times P_{e,h}}{SCOP \times (3.6 \times 10^6)} \right) (1+i)^{m-1} \tag{12}$$

with $Q_c^{(ref)}(m)$ and $Q_h^{(ref)}(m)$ being the cooling and heating loads, respectively, for the reference roofs in the time period m.

Then,

$$PW_m(C_e^{(ref)}(m)) - PW_m(C_e(m))$$

is the energy cost differential for period m between the reference and the retrofitted roofs.

When the NCS is positive, it means that the use of the retrofit measure on the roof generates cost savings compared to the reference case.

It is worth noting that energy consumption varies from year to year due to the aging phenomenon. Consequently, expression (11) cannot be reduced to a singular analytical representation as usually found in the literature [19].

In [51], the payback period (PB) is defined as the time t at which the NCS becomes zero. Since the coefficients in the series presented in (11) change with each time step m, the payback period t is determined by computing the cumulative net savings over each time horizon, m_0, as follows:

$$NCS(m_0) = \sum_{m=1}^{m_0} \left[PW_m(C_e^{(ref)}(m)) - PW_m(C_e(m)) \right] - C_M - C_I. \tag{13}$$

Then, if $NCS(m_0) < 0$ and $NCS(m_0 + 1) > 0$, the payback time t is estimated using the formula

$$t = m_0 - \frac{NCS(m_0)}{NCS(m_0 + 1) - NCS(m_0)}. \tag{14}$$

This value of t obtained from (14) is in agreement with the predominant value usually found in the literature [19,49], which usually assume that energy consumption is constant for all years.

2.7. Economics Indicators

The variables used for the economic computations in the LCCA are detailed in Table 3.

Table 3. Economic variables for the LCCA.

Variable	Value	Units
EPS cost	116	€/m^3
Insulation installation cost	13.15	€/m^2
Cool paint cost	9.45	€/m^2
Washing cost	1.63	€/m^2
Bituminous paint cost	8.01	€/m^2
Bituminous paint maintenance	0.4	€/m^2 yearly
Electricity cost	0.2403	kWh
Energy inflation rate	1.5–3.0–6.0	%
Discount rate	1.0–1.5–3.0	%
Lifetime	20	years

The cost of installing the combined retrofit measure on the roof and its maintaining are sourced from [50]. The electricity price is determined as the price in Spain, which includes taxes, for household consumers, as defined in reference [52]. Following the approach detailed in [53], three different sets of values for energy inflation and discount rates have been explored, as indicated in Table 3. Lastly, the maintenance discount rate i_M is assumed to be equal to dr, based on the assumption that the evolutions of both indices are closely aligned.

As for the conditioning equipment, our working assumption is that conditioning is invariably performed by an air-conditioning pump exclusively powered by electricity. Considering the relatively low buying capacity of the home occupants, we have chosen air conditioning units of mid-range quality with an A++ energy rating in line with European regulations. This selection is based on the common understanding that these devices are often priced lower than those carrying an A+++ energy certification. The efficiency parameters for the conditioning equipment are established at SEER = 3.4 for cooling and SCOP = 3 for heating. These pump efficiency values represent the averages of the values outlined in EU Regulation 626/2011 [54] for air conditioning equipment classified as A++.

3. Results and Discussion

3.1. Energy Results

Within this current section, the findings regarding the energy effectiveness of the roof retrofit proposal are presented for the case study mentioned above. The heating, cooling, and total loads generated by the heat flux through the reference and the retrofitted roofs are computed for each year of the LCCA whole time period. Then, the loads are compared, and energy savings estimates are obtained for each year and for the entire LCCA span time.

To perform analysis, the heat flux per unit area of the roof surface for the complete year is calculated, taking into consideration the hourly climatic data available in the weather files specific to Seville, as previously described. Then, when this flux is incoming, as happens in the cooling season, the flux is computed as cooling load, and when the heat flux goes out, as happens in the heating season, the flux is computed as heating load. The addition of the cooling and heating loads provides the total flux.

In these computations, as mentioned above, two protocols for cool roof maintenance have been considered: no washing and quinquennial power washing of the outer elastomeric paint.

In Figure 7a, the yearly heating, cooling, and total loads by m² of retrofitted roof are shown for the case of no washing of the cool coating. It can be observed that as a result of the high initial values of the cool-coating solar reflectivity, the values of the heating loads are higher in the first two years than for the remaining years due to the solar gain penalty; on the contrary, for the first two years, the cooling loads are lower than for the remaining years for the same reason. Regarding the total loads, this opposing behavior of the cooling and heating loads produces a final result that must be estimated considering the effect on the loads of the aging pattern. For the case study considered, the results depict a trend where total loads are notably higher in the first two years and then maintain a stable course in the remaining years.

It should be noted that the heating loads in the present case study are higher than the cooling loads for the whole LCCA time span, in line with the effect that the high solar reflectivity produces in the thermal flux through the roof. In Figure 7b, the yearly heating, cooling and total loads by m² of retrofitted roof are shown for the case of a periodic quinquennial wash of the cool coating. The first observation that can be made from this figure is how the quinquennial washing of the roof produces a cyclic behavior of the loads, which is very similar for each five-year period between two consecutive washes. As can be seen, the effect of the cool paint on decreasing solar gain produces lower values for the cooling loads than for the heating loads throughout the 20 years of the considered life-cycle time span.

It is worth noting that when the solar reflectivity of the cool paint reaches its highest values, that is, in the initial year, and then, after the quinquennial washing, years 6, 11, and 16, the cooling load reaches its minimum values; after each of these years, cooling loads are gradually increasing in each time interval between two consecutive washings, in line with the increasing loss of solar reflectivity produced by the aging effect of the cool paint. For the heating load, the pattern is just the opposite: when the solar reflectivity is maximum in years 1, 6, 11, and 16, the heating loads are maximum in accordance with the lowest values of solar gain; then, in the following years, the heating load follows a decreasing pattern produced by the aging effect that causes a loss of reflectivity and an increase in solar gain.

This opposing behavior in the cooling and heating loads produces a certain balance in all the years except for the initial year of each inter-washing time period. In these initial years, the predominant effect is the reduction of solar gain, so that the rise in heating load is not balanced by the reduction in cooling load, resulting in an increase in the total load for those years. For the remaining years of each period between washings, it is observed that the variations in cooling and heating loads caused by the effect of the aging of the cold layer are approximately compensated for by each other, producing a very small variation of the loads over the different years of each period.

On the other hand, the calculation of the heat flux for the reference roof gives a heating load equal to 28.72 kWh/m² and a cooling load equal to 38.32 kWh/m², which implies a total load equal to 67.04 kWh/m² for every year of the LCCA span time. By comparing these values with the loads for the retrofitted roof shown in Figures 7 and 8, it can be stated that the heating, cooling, and total loads for the retrofitted roof have lower values than the same loads for the reference roof, and this is. the case for all the years of the LCCA time span and for the two washing protocols considered; consequently, it can be stated that the retrofitted roof yields positive energy savings for all the years of the considered LCCA time span, as can be seen in Figure 9.

In Figure 8, the loads for the entire LCCA time span are shown for the reference and retrofitted roofs. According to Figure 7 and the subsequent discussion for heating and cooling loads and thus for the total load, the retrofitted roof exhibits lower values than the reference roof and, as can be appreciated in the figure, the highest reduction is achieved for the cooling loads. In Table 4, the values of the different loads for the LCCA span are shown for the retrofitted and reference roofs.

Table 4. Life-cycle loads and energy savings kWh/m².

	Heating Load	Cooling Load	Total Load	Total Energy Saving
Reference roof	574.35	766.56	1340.91	-
Retrofitted roof (No wash)	269.23	103.03	365.29	975.62
Retrofitted roof (Quinq. wash)	280.23	90.27	370.51	970.40

(**a**)   (**b**)
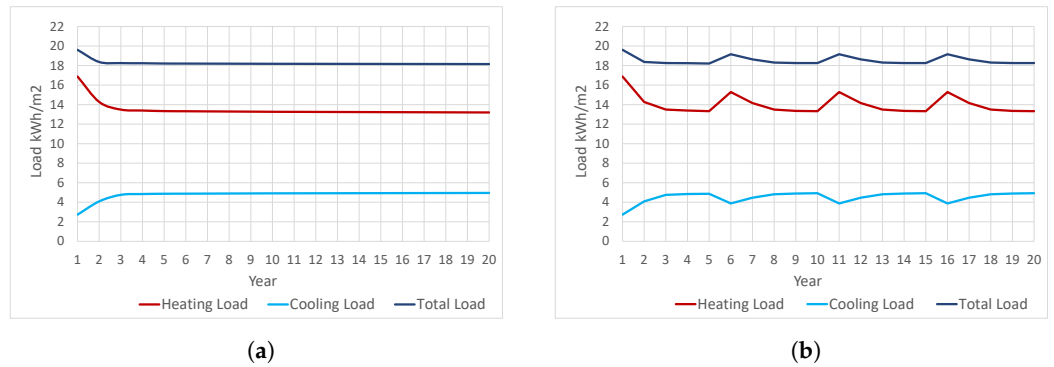
Figure 7. Yearly heating, cooling, and total loads for the retrofitted roof with (**a**) no wash of the cool coating; (**b**) quinquennial wash of the cool coating.
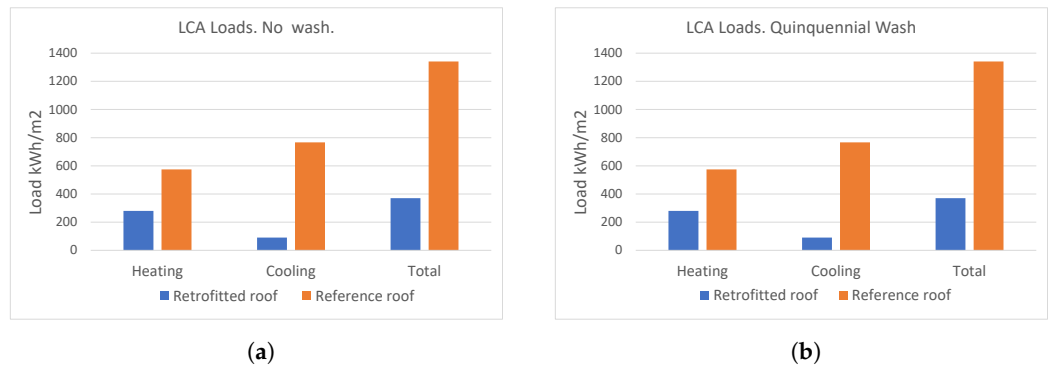

(**a**)   (**b**)

Figure 8. LC heating, cooling, and total loads for the reference and retrofitted roofs with (**a**) no wash of the cool coating; (**b**) quinquennial wash of the cool coating.
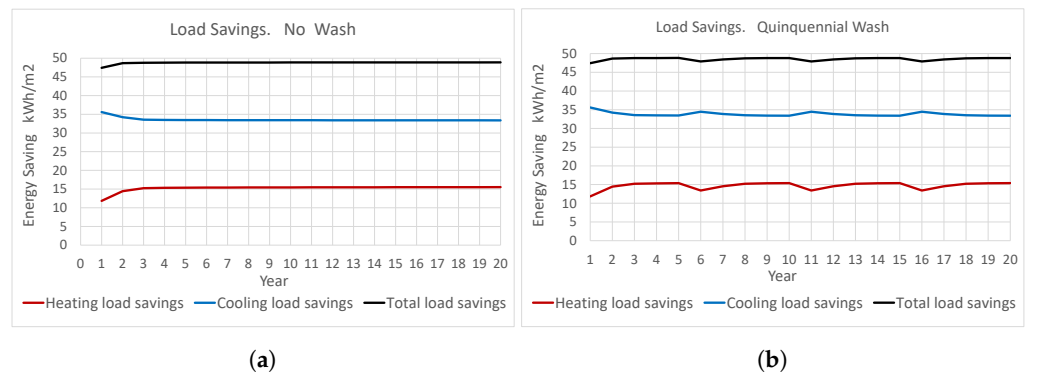

(**a**)   (**b**)

Figure 9. Yearly heating, cooling, and total energy savings for the retrofitted and the reference roofs for (**a**) no wash of the cool coating; (**b**) quinquennial wash of the cool coating.

The energy savings for each specific load are defined as the difference between the load for the reference roof and the load for the retrofitted roof. Thus, positive energy savings mean that the load on the reference roof is higher than the same load on the retrofitted roof. As can be observed in Table 4, the retrofitted roof has positive or true total energy savings

when compared to the reference case. In Figure 9, the heating, cooling, and total savings are displayed for each year of the LCCA span time.

It can be noted that the case of periodic quinquennial wash of the cool coating provides slightly better results with respect to the total load and energy savings compared to the case of no wash.

According to the above discussion, for the case of no wash of the cool coating, Figure 9a, the lowest values for the energy savings are obtained in the two initial years and then tend to stabilize for the remaining years. It should be noted that the savings for cooling load are much higher than the savings for heating load.

In Figure 9b, the load savings for the case of a quinquennial wash of the cool coating are shown. It can be observed that the lowest values for the energy savings are obtained in the two initial years and then in the years in which the washing is carried out due to the penalty in the solar gain produced by the high values of solar reflectivity. For the remaining years of each period, the decrease in the solar reflectivity produced by the aging lowers the solar reflectivity and, as can be seen in the figure, this makes the total load go down.

Likewise, in Figure 9, the greatest effect in producing savings is observed for the cooling load when compared to the heating load, as a result of the decision to install a cool paint with very reduced solar reflectivity.

Finally, in Table 5, the LCCA energy savings are shown for all housing in every district of the neighborhood and the neighborhood as a whole.

Table 5. Life cycle energy savings for the districts and neighborhood as a whole.

District	No Wash		Quinquennial Wash	
A	21,796,326.4	kWh	21,679,684.1	kWh
B	22,781,702.6	kWh	22,659,787.1	kWh
C	24,696,844.7	kWh	24,564,680.3	kWh
D	22,923,167.5	kWh	22,800,494.9	kWh
E	16,911,397.1	kWh	16,820,896.3	kWh
All	109,109.44	mWh	108,525.54	[] mWh

Taking into account the assumed SEER and SCOP coefficients, the savings in thermal loads shown in Table 5 are equivalent to a total reduction in energy consumption of 32,500 mWh for the entire neighborhood and the entire life cycle, which is equivalent to a 72% reduction in energy consumption to achieve indoor thermal comfort. This value of energy consumption decrease implies a total reduction in CO_2 emissions of 4488.31 tons.

3.2. LCCA Results

In this section, the net savings and payback periods are used as performance indicators to perform the LCCA. Due to the investment in refurbishment made compared to the reference case, the NCS and PB are assessed under the economic framework described previously and considering the impact on energy loads of the effect of aging as described previously.

In Table 6, the monetary net savings per unit of roof surface area, NCS, and the payback period, PB, are shown for the two maintenance protocols considered: no powerful wash during the entire LCCA time period and a periodic quinquennial wash. Additionally, net savings are presented for the roof with three standard surface areas in the framework of social housing, that is, roof areas equal to 60, 70, and 80 m^2: the usual range of roof surfaces for this kind of dwelling.

Table 6. Life-cycle monetary savings and associated payback periods.

				NCS [€] for roof surface		
				No Wash		
i	dr	NCS [€/m^2]	PB [years]	60 m^2	70 m^2	80 m^2
0.015	0.01	57.26	7.69	3435.6	4008.2	4580.8
0.03	0.015	64.96	7.15	3897.6	4547.2	5196.8
0.06	0.03	77.18	6.84	4630.8	5402.6	6174.4
			Quinquennial Wash			
				NCS [€] for roof surface		
i	dr	NCS [€/m^2]	PB [years]	60 m^2	70 m^2	80 m^2
0.015	0.01	52.45	8.12	3147	3671.5	4196
0.03	0.015	60.03	7.42	3601.8	4202.1	4802.4
0.06	0.03	72.026	6.93	4321.56	5041.82	5762.08

As can be seen in Table 6, the proposed retrofitting measures are cost-efficient for all the cases analyzed. However, it can be stated that the results obtained for the no-wash maintenance protocols are better than those obtained for the quinquennial washing, with higher values of monetary savings and thus shorter PB periods for the no wash case. It should be highlighted that the payback periods for all the cases are not long and range between 6.84 and 8.12 years. These can be considered reasonable time intervals to recover the investment made in the retrofitting.

Regarding the economic indicators, it can be observed that the proposed combined retrofit measure yields the highest monetary savings for high values of the energy inflation index and the monetary discount rate represented here by i = 6% and dr = 3%. Taking into consideration the present economic situation characterized by very high energy price growth and very high inflation rates, it can be concluded that, financially speaking, the proposed retrofitting measure is highly effective.

In the same table, net monetary savings are presented for three typical roof areas of social dwellings. As can be observed, the value of these savings is relevant, and their impact on the household economy of regular residents of social housing, usually characterized by low incomes, can be described as of great significance and with a high potential to achieve indoor comfort and health conditions and reduce the high rates of energy poverty found among the inhabitants of this type of housing.

Finally, in Table 7, the monetary savings for the whole LCCA time span for all the retrofitted dwellings in each district and for the entire neighborhood are shown for all the different economic scenarios of energy inflation and discount rate considered.

Table 7. Net savings [€] for the districts and the entire neighborhood. The values of i and dr are given in %.

District	No Wash			Quinquennial Wash		
	i = 1.5, d = 1	i = 1, d = 1.5	i = 6, d = 3	i = 1.5, d = 1	i = 1, d = 1.5	i = 6, d = 3
A	1,279,245.66	1,451,271.36	1,724,278.38	1,171,785.45	1,341,130.23	1,609,222.23
B	1,337,078.26	1,516,880.96	1,802,230.18	1,224,759.95	1,401,760.53	1,681,972.53
C	1,449,479.64	1,644,397.44	1,953,734.52	1,327,719.30	1,519,599.42	1,823,367.42
D	1,345,380.96	1,526,300.16	1,813,421.28	1,232,365.20	1,410,464.88	1,692,416.88
E	992,544.84	1,126,016.64	1,337,838.12	909,168.30	1,040,560.02	1,248,568.02
All	6,403,729.36	7,264,866.56	8,631,502.48	5,865,798.20	6,713,515.08	8,055,547.08

As can be observed, the quantities saved during the analysis period, the life-cycle time span, are significant for all the analyzed scenarios in terms of both economy and maintenance protocols. It is observed that for the entire neighborhood, quantities saved

range from €6.4 million to over €8.6 million in the no wash case, depending on the economic scenario.

4. Conclusions

In this work, the Aura Strategy as an intervention methodology to find global solutions to issues in outdated neighborhoods has been visualized through the analysis of a constructive solution to improve the energy performance of the roofing of buildings applied to the case study of an energy obsolete residential neighborhood in the city of Seville, Spain.

This architectural solution impacts 3 out of the 4 lines of intervention: Health and Comfort, Materiality, Cultural Identity, and Energy and Conditioning that the Aura Strategy proposes as the focus of all urban regeneration interventions.

1. Energy and Conditioning: the effectiveness of the proposed retrofit measure, which combines a cold coating with insulation to reduce energy loads and achieve indoor comfort in the affected dwellings, is confirmed. For the LCCA time span, the load reduction reaches 975.62 kWh/m^2 for the maintenance protocol without washing and 970.40 kWh/m^2 for the maintenance protocol with five-yearly washing. When these savings are quantified for all homes with roofs in the neighborhood, the results are 109,109.44 and 108,525.54 mWh, respectively. These thermal load reduction results indicate a 72% reduction in energy consumption to achieve indoor thermal comfort. This load reduction is equivalent to a savings of almost 4,488 tons of greenhouse gas emissions across the district and over the entire lifetime of the applied roof retrofit measure. Therefore, it can be concluded that the implementation of the proposed retrofit measure to reduce energy consumption leads to significant energy saving capacity.

2. Materiality: From a financial perspective, the Life Cycle Cost Analysis provides net economic cost savings for the entire analysis period. In the case of the No-wash maintenance protocol, these range between 57.26 and 77.18 €m^2 per dwelling, depending on the economic scenario, with return-on-investment periods between 7.69 and 6.84 years. In the case of the Quinquennial Wash maintenance protocol, net savings are between 52.45 and 72.03 €/m^2 and return-on-investment periods are between 8.12 and 6.93 years. This allows us to establish the cost effectiveness of the proposed retrofit measure for family dwellings and homeowners. If all affected homes in the neighborhood are considered, financial savings for the LCCA time span range from €5,865,798.20 to €8,055,547.08 in the case of the quinquennial wash maintenance protocol, and from €6,403,729.36 to €8,631,502.48 in the case of the no-wash maintenance protocol. Therefore, financially speaking, the economic viability of the proposed retrofitting is confirmed, as well as the significant savings that its implementation implies for individual households and for the neighborhood as a whole.

3. Health and Comfort: The applied solution, by incorporating thermal insulation in the roof, improves indoor comfort conditions in the affected dwellings. The proposal, in addition to the consequent reduction of energy expenditure and consequently the reduction of economic expenditure, implies the reduction of energy poverty levels, the improvement of indoor living conditions, and their repercussions on health and well-being [55]. It also implies a very positive effect on the reduction of greenhouse gas emissions.

In short, this retrofit proposal fulfills the premises established by the Aura Strategy: the regeneration of obsolete neighborhoods through specific energy retrofit interventions that offer global benefits to the population of the case study, as described in this article. In turn, this has a direct impact on people's health, especially among elderly residents in the neighborhood, and on the fight against climate change.

To put these figures in context, it should be highlighted that in 2018, the annual income per capita in the Polígono de San Pablo was €8128.86 while the household income was €19,973.84 (Source: National Institute of Statistics, Spain). Thus, savings would constitute a significant percentage of the economic capacity of residents of the neighborhood.

The energy and economic results obtained from the numerical modeling at the roof building level are consistent with the previous literature. On the other hand, the specific solution adopted for roof retrofitting in the research carried out has benefited from previous studies carried out by the authors, which has allowed the high levels of energy savings presented in this study that have contributed, in the context of the Aura Strategy, to the finding of significant energy and monetary savings at the neighborhood level.

The main limitation of this study was the scarcity of social information related to the evaluation of the application of the research results by all parties involved in society, such as tenants, municipalities, state governments and other subjects, both private and public, with the possibility of influencing the decision making process leading to the implementation of the rehabilitation measures described above, especially the subsidization of the necessary investments.

Therefore, the possibility of extending the present research to the study of the social response to the type of strategies proposed in the present investigation represents an opportunity for new studies that also need to be addressed.

Finally, the study focuses on the analysis of a specific constructive solution to improve the thermal performance of the roof of a typical building. The results obtained with this initial approach have certain limitations, suggesting the possibility of extending the research carried out by comparing it with other construction alternatives.

References

1. Herrera-Limones, R.; León-Rodríguez, Á.; López-Escamilla, Á. Solar Decathlon Latin America and Caribbean: Comfort and the Balance between Passive and Active Design. *Sustainability* **2019**, *11*, 3498. [CrossRef]
2. Herrera-Limones, R.; Hernández-Valencia, M.; Roa-Fernández, J. Urban regeneration through retrofitting social housing: The AURA 3.1 prototype. *J. Hous. Built Environ.* **2023**, *38*, 837–859. [CrossRef]
3. Catalogue of Vulnerable Neighborhoods (BV) in Spain 2011 (Ministry of Transport, Mobility and Urban Agenda. Universidad Politécnica de Madrid v. 05/2021). Available online: bhttps://cdn.mitma.gob.es/portal-web-drupal/vivienda/barrios-vunerables/bbvv-2011-01-andalucia.pdf (accessed on 20 January 2023).
4. Berdahl, P.; Bretz, S.E. Preliminary survey of the solar reflectance of cool roofing materials. *Energy Build.* **1997**, *25*, 149–158. [CrossRef]
5. Kim, H.; Gu, D.; Kim, H.Y. Effects of Urban Heat Island mitigation in various climate zones in the United States. *Sustain. Cities Soc.* **2018**, *41*, 841–852. [CrossRef]
6. Domínguez-Delgado, A.; Domínguez-Torres, H.; Domínguez-Torres, C.A. Energy and Economic Life Cycle Assessment of Cool Roofs Applied to the Refurbishment of Social Housing in Southern Spain. *Sustainability* **2020**, *12*, 5602. [CrossRef]
7. Mazzeo, D.; Kontoleon, K.J. The role of inclination and orientation of different building roof typologies on indoor and outdoor environment thermal comfort in Italy and Greece. *Sustain. Cities Soc.* **2020**, *60*, 102111. [CrossRef]
8. Hamdan, M.A.; Yamin, J.; Hafez, E.M.A. Passive cooling roof design under Jordanian climate. *Sustain. Cities Soc.* **2012**, *5*, 26–29. [CrossRef]
9. Kolokotsa, D.; Giannariakis, G.; Gobakis, K.; Giannarakis, G.;Synnefa, A.; Santamouris, M. Cool roofs and cool pavements application in Acharnes, Greece. *Sustain. Cities Soc.* **2018**, *37*, 466–474. [CrossRef]
10. Testa, J.; Krarti, M. Evaluation of energy savings potential of variable reflective roofingsystems for US buildings. *Sustain. Cities Soc.* **2017**, *31*, 62–73. [CrossRef]
11. Anand, J.; Sailor, D.; Baniassadi, A. The relative role of solar reflectance and thermal emittance for passive daytime radiative cooling technologies applied to rooftops. *Sustain. Cities Soc.* **2021**, *65*, 102612. [CrossRef]

12. Pisello, A.L. Thermal-energy analysis of roof cool clay tiles for application in historic buildings and cities. *Sustain. Cities Soc.* **2015**, *19*, 271–280. [CrossRef]

13. Guerrero Delgado, M.C.; SÁnchez Ramos, J.; Palomo Amores, T.R.; Castro Medina, D.; Álvarez Domínguez, S. Improving habitability in social housing through passive cooling: A case study in Mengíbar (Jaén, Spain). *Sustain. Cities Soc.* **2022**, *78*, 103642. [CrossRef]

14. Herath, P.; Thatcher, M.; Jin, H.; Bai, X. Effectiveness of urban surface characteristics as mitigation strategies for the excessive summer heat in cities. *Sustain. Cities Soc.* **2021**, *72*, 103072. [CrossRef]

15. Athmani, W.; Sriti, L.; Dabaieh, M.; Younsi, Z. The Potential of Using Passive Cooling Roof Techniques to Improve Thermal Performance and Energy Efficiency of Residential Buildings in Hot Arid Regions. *Buildings* **2023**, *13*, 21. [CrossRef]

16. Nutakki, T.U.K.; Kazim, W.U.; Alamara, K.; Salameh, T.; Abdelkareem, M.A. Experimental Investigation on Aging and Energy Savings Evaluation of High Solar Reflective Index (SRI) Paints: A Case Study on Residential Households in the GCC Region. *Buildings* **2023**, *13*, 419. [CrossRef]

17. Younes, J.; Ghali, K.; Ghaddar, N. Diurnal Selective Radiative Cooling Impact in Mitigating Urban Heat Island Effect. *Sustain. Cities Soc.* **2022**, *83*, 103932. [CrossRef]

18. Elnabawi, M.H.; Alhumaidi, A.; Osman, B.; Alshehhi, R. Cool Roofs in Hot Climates: A Conceptual Review of Modelling Methods and Limitations. *Buildings* **2022**, *12*, 1968. [CrossRef]

19. Saafi, K.; Daouas, N. A life-cycle cost analysis for an optimum combination of cool coating and thermal insulation of residential building roofs in Tunisia. *Energy* **2018**, *152*, 925–938. [CrossRef]

20. Domínguez-Torres, C.A.; Domínguez-Torres, H.; Domínguez-Delgado, A. Optimization of a Combination of Thermal Insulation and Cool Roof for the Refurbishment of Social Housing in Southern Spain. *Sustainability* **2021**, *13*, 10738. [CrossRef]

21. *NBSSIR 83-2655*; Thermal Analysis Research Program Reference Manual. National Bureau of Standards: Gaithersburg, MD, USA, 1983; p. 21.

22. Clark, G.; Allen, C. The Estimation of Atmospheric Radiation for Clear and Cloudy Skies. In Proceedings of the 2nd National Passive Solar Conference (AS/ISES), Philadelphia, PA, USA, 16–18 March 1978; pp. 675–678.

23. *Energy Plus Software 9.1.0*; U.S. Department of Energy (DOE). Building Technologies Office (BTO). University of Illinois, USA. Available online: https://energyplus.net/downloads (accessed on 14 March 2023).

24. Hagishima, A.; Tanimoto, J. Field measurements for estimating the convective heat transfer coefficient at building surfaces. *Build. Environ.* **2003**, *38*, 873–881. [CrossRef]

25. Gagliano, A.; Nocera, F.; Aneli, S. Thermodynamic analysis of ventilated façades under different wind conditions in summer period. *Energy Build.* **2016**, *122*, 131–139. [CrossRef]

26. Hickson, R.I.; Barry, S.I.; Mercer, G.N.; Sidhu, H.S. Finite difference schemes for multilayer diffusion. *Math. Comput. Model.* **2011**, *54*, 210–220. [CrossRef]

27. American Society of Heating, Refrigerating and Air Conditioning Engineers Inc. *ASHRAE Fundamentals Handbook (S.I.)*; American Society of Heating, Refrigerating and Air Conditioning Engineers Inc.: Atlanta, GA, USA, 1997.

28. Dominguez-Torres, C.A.; Suarez, R.; León-Rodríguez, A.L.; Domínguez-Delgado, A. Experimental validation of a dynamic numeric model to simulate the thermal behavior of a facade. *Appl. Therm. Eng.* **2022**, *204*, 1359–4311. [CrossRef]

29. De Masi, R.F.; Ruggiero, S.; Vanoli, G.P. Acrylic white paint of industrial sector for cool roofing application: Experimental investigation of summer behavior and aging problem under Mediterranean climate. *Sol. Energy* **2018**, *169*, 468–487. [CrossRef]

30. Mastrapostoli, E.; Santamouris, M.; Kolokotsa, D.; Vassilis, P.; Venieri, D.; Gompakis, K. On the ageing of cool roofs: Measure of the optical degradation, chemical and biological analysis and assessment of the energy impact. *Energy Build.* **2016**, *114*, 191–199. [CrossRef]

31. Xue, X.; Yang, J.; Zhang, W.; Jiang, L.; Qua, J.; Xu, L.; Zhang, H.; Song, J.; Zhang, R.; Li, Y.; et al. The study of an energy efficient cool white roof coating based on styrene acrylate copolymer and cement for waterproofing purpose. Part I: Optical properties, estimated cooling effect and relevant properties after dirt and accelerated exposures.*Constr. Build. Mat.* **2015**, *98*, 176–184. [CrossRef]

32. Allen Zielnik, A. Durability, pausing for reflection on aging of the cool roof. *J. Archit. Coat.* **2008**, 63–65. Available online: https://www.paintsquare.com/library/articles/Durability (accessed on 17 January 2023).

33. Bretz, S.E.; Akbari, H. Long-term performance of high-albedo roof coatings. *Energy Build.* **1997**, *25*, 159–167. [CrossRef]

34. Eilert, P. *High Albedo (Cool) Roofs: Codes and Standards Enhancement (CASE) Study*; Pacific Gas and Electric Company: San Francisco, CA, USA, 2000. Available online: https://www.everglow.us/pdf (accessed on 10 January 2023).

35. Prontuario de Soluciones Constructivas del CTE. Instituto de Ciencias de la Construcción Eduardo Torroja. Available online: http://cte-web.iccl.es/materiales.php (accessed on 12 March 2020).

36. Pedro Fernández Díaz. Centrales Térmicas. Biblioteca sobre Ingeniería Energética. Universidad de Cantabria. Available online: https://pfernandezdiez.es/es/libro?id=15 (accessed on 15 March 2020).

37. Agencia Estatal de Meteorología de España. *Guía Resumida del Clima en España (1981–2010)*; Agencia Estatal de Meteorología de España: Madrid, Spain, 2010.

38. Auliac, S.; Le Hyaric, A.; Morice, J.; Hecht, F.; Ohtsuka, K.; Pironneau, O. *FreeFem++*, Version 3.31-2, 3rd ed.; Inria: Paris, France, 2017. Available online: http:www.freefem.orgr (accessed on 11 June 2023).

39. Çengel, Y. *Heat and Mass Transfer. A Practical Approach*, 3rd ed.; McGraw Hill: New York, NY, USA, 2007.

40. Gentle, A.R.; Aguilar, J.L.C.; Smith, G.B. Optimized cool roofs: Integrating albedo and thermal emittance with R-value. *Sol. Energy Mater. Sol. Cells* **2011**, *95*, 3207–3215. [CrossRef]

41. Rossi, M.; Rocco, V.M. External walls design: The role of periodic thermal transmittance and internal areal heat capacity. *Energy Build.* **2014**, *68*, 732–740. [CrossRef]

42. Al-Sanea, S.A.; Zedan, M.F.; Al-Ajlan, S.A. Effect of electricity tariff on the optimum insulation-thickness in building walls as determined by a dynamic heat-transfer model. *Appl. Energy* **2005**, *82*, 313–330. [CrossRef]

43. Ozel, M. Effect of wall orientation on the optimum insulation thickness by using a dynamic method. *Appl. Energy* **2011**, *88*, 2429–2435. [CrossRef]

44. Daouas, N. Impact of external longwave radiation on optimum insulation thickness in Tunisian building roofs based on a dynamic analytical model. *Appl. Energy* **2016**, *177*, 136–148. [CrossRef]

45. Yuan, J.; Farnham, C.; Emura, K.; Alam, M.A. Proposal for optimum combination of reflectivity and insulation thickness of building exterior walls for annual thermal load in Japan. *Build. Environ.* **2016**, *103*, 228–237. [CrossRef]

46. Arumugam, R.S.; Garg, V.; Ram, V.V.; Bhatia, A. Optimizing roof insulation for roofs with high albedo coating and radiant barriers in India. *J. Build. Eng.* **2015**, *2*, 52–58. [CrossRef]

47. Synnefa, A.; Saliari, M.; Santamouris, M. Experimental and numerical assessment of the impact of increased roof reflectance on a school building in Athens. *Energy Build.* **2012**, *55*, 7–15. [CrossRef]

48. Reglamento de Instalaciones Térmicas en los Edificios. Ministerio para la Transición Ecológica y el Reto Demográfico. Available online: https://energia.gob.es/desarrollo/EficienciaEnergetica/RITE/Paginas/InstalacionesTermicas.aspx (accessed on 23 March 2023).

49. Duffie, J.A.; Beckman, W. *Solar Engineering of Thermal Processes*; John Wiley and Sons Inc.: Hoboken, NJ, USA, 2006.

50. CYPE Engineers. CYPE Ingenieros Construction Price Generator. 2017. Available online: http://www.generadordeprecios.info/gsc.tab=0 (accessed on 28 March 2023).

51. Vincelas, F.F.C.; Ghislain, T.; Robert, T. Influence of the types of fuel and building material on energy savings into building in tropical region of Cameroon. *Appl. Therm. Eng.* **2017**, *122*, 806–819. [CrossRef]

52. Available online: https://ec.europa.eu/eurostat/statistics-explained/index.php/Natural-gas-price-statistics (accessed on 22 March 2022).

53. Nydahl, H.; Andersson, S.; Astrand, A.P.; Olofsson, T. Including future climate induced cost when assessing building refurbishment performance. *Energy Build.* **2019**, *203*, 109428. [CrossRef]

54. Commission Delegated Regulation (EU) No 626/2011 of 4 May 2011 Supplementing Directive 2010/30/EU of the European Parliament and of the Council with regard to Energy Labelling of Air Conditioners. Available online: https://eur-lex.europa.eu/legal-content/en/ALL/?uri=CELEX%3A32011R0626 (accessed on 12 February 2023.)

55. Clavijo-Núñez, S.; Herrera-Limones, R.; Rey-Pérez, J.; Torres-García, M. Energy poverty in Andalusia. An analysis through decentralised indicators. *Energy Policy* **2022**, *167*, 113083. [CrossRef]